Long Duration Overvoltages due to Current Backfeeding in Secondary Networks

Reynaldo Salcedo, *Student Member, IEEE*, Xuanchang Ran, Francisco de León, *Senior Member, IEEE*, Dariusz Czarkowski, *Member, IEEE*, and Vitaly Spitsa, *Member, IEEE*

***Abstract*—This paper analyzes long duration overvoltages due to backfeeding currents from the low-voltage network to the medium-voltage network through network protectors in heavily meshed underground distribution networks. Overvoltages above 3 p.u. may be developed as a result of a simultaneous occurrence of three phenomena: neutral displacement, Ferranti effect, and current chopping. A detailed model of a typical distribution network is utilized for the study. Time-domain simulations are performed using an Electromagnetic Transients Program-type program. The results demonstrate that overvoltages due to backfeeding last longer during peak load operating conditions, and the largest peak overvoltages occur at no load.**

***Index Terms*—Metropolitan area networks, overvoltages, power system transients, time-domain analysis.**

I. Introduction

OVERVOLTAGES in distribution networks may arise because of switching transients, resonance, lightning strikes, and ground faults among other causes [1]. Due to strict requirements of electrical power quality and reliability in urban areas, secondary grid networks are often heavily meshed and interconnected by means of network protectors [low-voltage (LV) circuit breakers], the operation of which prevents the continuous flow of reverse power [1]–[4]. There are three modes of operation for the network protectors: sensitive, time delayed, and insensitive. During an unbalanced fault, such as a single-line-to-ground (SLG) fault, on the medium-voltage (MV) side, large overvoltages may occur at the unfaulted phases. Although all of the network protectors "see" the fault at the same time, they do not operate simultaneously. Many of them open very quickly with opening times similar to those of the feeder breaker. However, some operate a few cycles later, others take several seconds to open, and a few might even fail to operate. Therefore, depending on the settings of the network protectors, overvoltages can last a significantly long time due to backfeeding of current from the LV network into the fault at the MV network. A comprehensive literature review [8]–[21] revealed that although this phenomenon has been considered, it has not been studied and documented in depth.

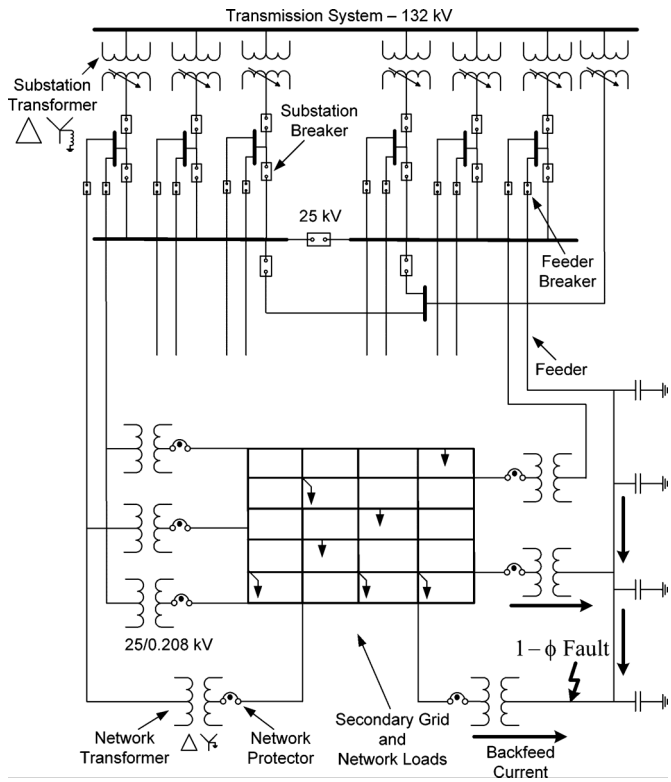

Fig. 1. Typical configuration of the underground distribution network.

Analysis of overvoltages in distribution networks is of high importance since they may damage the power system infrastructure and the customer electrical equipment. The scenarios studied in this paper indicate that overvoltage stresses are imposed on insulation, microprocessor-controlled equipment, and switching devices by overvoltages during backfeeding. Fig. 1 shows a schematic diagram of the network under analysis. The network design assumes a classical secondary grid of the distribution network described in [1] and [4]. Our modeling methods have been exhaustively validated against field measurements as reported in [4]–[7].

Many published studies exist regarding overvoltages in electrical distribution systems. Some of them consider the overvoltage impact caused by distributed generation [8]–[10]. Others address overvoltage phenomena due to lightning in LV systems, including the electrical stresses imposed on cable sections [11]–[16]. There are studies on overvoltages due to device switching, harmonic resonances, power system restoration, and

Manuscript received March 07, 2013; revised May 29, 2013; accepted July 16, 2013. Date of publication August 15, 2013; date of current version September 19, 2013.This work was supported by the GAANN Fellowship from the U.S. Department. Paper no. TPWRD-00265-2013.

R. Salcedo, X. Ran, F. de León, and D. Czarkowski are with the Electrical and Computer Engineering Department, Polytechnic Institute of New York University, Brooklyn, NY 11201 USA (e-mail: reynal74@aol.com; xuanchangran@hotmail.com; fdeleon@poly.edu; dcz@poly.edu).

V. Spitsa is with the Electrical Engineering Department, San Jose State University, San Jose, CA 95192 USA (e-mail: vitaly.spitsa@sjsu.edu).

Digital Object Identifier 10.1109/TPWRD.2013.2273897

ground faults among other sources [17], [18]. In addition, some research has been presented on long duration overvoltages and its effects on the system [19]–[21]. In [19], a wide range of transient overvoltages and their origins is reviewed. A discussion on temporary overvoltages caused by a ground fault in a large radial MV network is presented in [20]. Finally, [21] provides the analysis and description of field test recordings for cable switching transients in 25-kV underground distribution systems. However, these studies deal only with voltage swells, steady-state overvoltages in radial distribution networks, or underground distribution networks without a heavily meshed secondary grid.

The original contribution of this paper is the methodological investigation of long duration overvoltages in heavily meshed underground distribution networks due to backfeeding current and the comparison of various mitigating techniques.

The study is carried out by dynamically simulating single-line-to-ground faults on a selected primary section located toward the end of a feeder. The network is studied under different loading conditions to establish a relationship between the overvoltage magnitude, its duration, and the network loading. Simulations were performed using the electromagnetic transient program (EMTP) [22].

II. Theoretical Considerations

The long duration transient overvoltages studied in this paper are caused by a simultaneous occurrence of three different phenomena: First, a neutral is displaced as a result of the single-line-to-ground fault on an MV feeder that is left floating; second, the far-end feeder voltage increases due to the capacitive charging of this feeder during the fault (Ferranti effect); and, finally, the fault current is chopped by the opening of the last network protector. The individual contributions of each one of these phenomena to the compounded long duration overvoltages are analyzed as follows.

A. Neutral Displacement During Single-Line-to-Ground Faults: Overvoltages Reaching 1.73 p.u.

As shown in Fig. 1, the substation is composed of step-down transformers connected delta-wye, grounded by means of reactors. During normal operation, its breakers are closed, and a reference to ground is present on the primary feeder sections as indicated in Fig. 2(a). When the single-line-to-ground fault occurs and the circuit breaker (CB) of the faulted feeder is still closed, the neutral shifts only a little because the substation transformers are grounded; see Fig. 2(b). However, when this breaker trips to clear the fault, the corresponding feeder becomes isolated from ground (except at the faulted point). Note that the faulted feeder is left floating since the primary of the network transformers is connected in delta. Therefore, the neutral is shifted to the center of a triangle having the reference on one corner. As a consequence, the line-to-ground voltage of the unfaulted phases becomes the line-to-line voltage of the system or 1.73 p.u. as shown in Fig. 2(c).

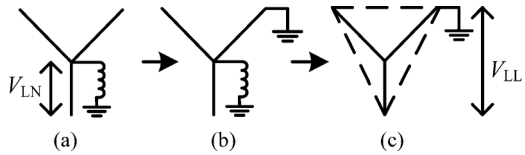

Fig. 2. Change from wye-grounded to delta due to a single-line-to-ground fault and breaker trip. (a) Prefault. (b) Fault before the breaker opens. (c) Fault after the breaker opens.

B. Mechanism of Backfeeding

According to the network architecture design shown in Fig. 1, when a feeder breaker opens to clear a fault or due to scheduled operations, the network protectors along the corresponding feeder should also trip to de-energize the feeder. A sequence of electrical transients is initiated at different parts of the network. For the present study, it was assumed that a single-line-to-ground fault occurs at some point along one of the MV feeders, which is a very common circumstance. Subsequently, the breaker attached to the faulted feeder trips stopping the fault current contribution from the area substation. After the feeder is isolated from the substation, the fault is solely sustained by reverse current (backfeeding) flowing from the secondary network to the faulted cable section through the network transformers. Since the primaries of the network transformers are connected in delta, the faulted feeder is left floating and the circulation of backfeeding current is through the capacitance to ground of the MV cables.

Ideally, the backfeeding through each transformer and associated network protector rapidly satisfies operational requirements for network protector tripping. This results in fast isolation of the faulted feeder which prevents cables sections, joints, fuses, and other equipment from being damaged. Furthermore, it allows maintenance crews to fix and re-energize the feeder fast. Since a minimum magnitude of reverse (active) power is needed for the network protectors to trip, the feeder length, fault location, and power rating of transformers play important roles in determining when these devices open. Upon isolation of the faulted feeder, its corresponding loading redistributes among remaining energized feeders. For operational reasons, such as to prevent the cycling of network protectors, some of them are "de-sensitized," producing much longer opening times.

C. Ferranti Effect: Overvoltages Exceeding 1.73 p.u. Due to Backfeeding Current Into Cable Capacitances

In contrast with overhead lines, underground cables have a large capacitance to ground. During backfeeding conditions (current flowing from secondary to primary), these cables behave as capacitive loads. When a single-line-to-ground fault occurs in systems similar to Fig. 1, voltages will increase beyond the line-to-line level due to the Ferranti effect. These overvoltages might reach or even exceed 2 p.u., depending on the capacitive charging power of the feeder and the system loading [23]. These conditions will persist until the last network protector along the faulted feeder trips.

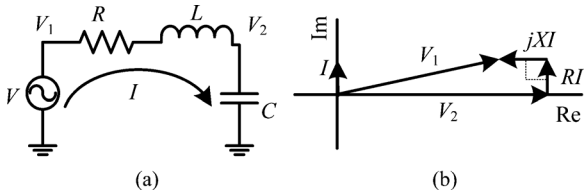

Fig. 3. Analysis circuit. (a) Simplification of the network. (b) Phasor diagram.

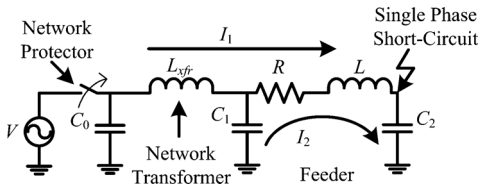

Fig. 4. Simplification of the network to illustrate current chopping.

For the purpose of analysis, consider the network shown in Fig. 3(a), where the voltage source R and L represent the equivalent of the faulted feeder, as seen from the secondary grid. C represents the cable capacitance. By means of the phasor diagram of Fig. 3(b), one can see that $|V_2| > |V_1|$ because of the current flowing into the capacitor.

D. Voltage Spike Caused by Current Chopping

As previously discussed, during a single-phase fault in a system, such as Fig. 1, there will be a neutral shift which causes line voltage to be observed on the primary side of the network transformers. Furthermore, as a result of the backfeeding current into the primary cable capacitances, the Ferranti effect might be present in the network depending on how heavily the network is loaded, raising the phase voltages to even higher values. At the instant the last connected network protector trips, the remaining part of the circuit experiences a large voltage spike which is produced as a result of the LV CB interrupting the backfeeding current near its zero crossing. A chopping current level of 0.5 A is assumed for the presented cases [24]. The magnitude of the spike may exceed more than twice the rated system voltage [24]. This is an outcome of the underdamped behavior exhibited by the circuit. Its simplified circuit diagram is given in Fig. 4. This circuit corresponds to the equivalent state of the faulted feeder before the opening of the last network protector, represented by the ideal switch in the figure.

E. Unbalanced Overvoltages for Single-Line-to-Ground Faults

In fault analysis, it is common practice to neglect resistive parts of branch impedances and perform calculations using reactances only. In such a case, calculated magnitudes of overvoltages in the unfaulted power system phases during a single-line-to-ground (SLG) fault are equal. However, this widely used assumption may be incorrect for distribution networks. They are characterized by a significantly higher R/X ratio than transmission systems. As shown hereafter, the resistive parts of the branch impedances should not be neglected in the overvoltage studies since they introduce significant imbalance of overvoltage magnitudes. To demonstrate this fact, one section of a three-phase branch shown in Fig. 5 is considered.

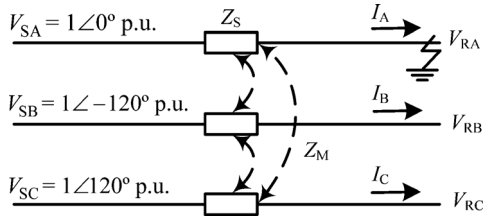

Fig. 5. Circuit diagram of a single-line-to-ground-fault at phase A.

The following matrix equation relates voltages and currents in the circuit (assuming continuous transposition):

$$\begin{bmatrix} \bar{V}_{\mathrm{RA}} \\ \bar{V}_{\mathrm{RB}} \\ \bar{V}_{\mathrm{RC}} \end{bmatrix} = \begin{bmatrix} \bar{V}_{\mathrm{SA}} \\ \bar{V}_{\mathrm{SB}} \\ \bar{V}_{\mathrm{SC}} \end{bmatrix} - \begin{bmatrix} \bar{Z}_S & \bar{Z}_M & \bar{Z}_M \\ \bar{Z}_M & \bar{Z}_S & \bar{Z}_M \\ \bar{Z}_M & \bar{Z}_M & \bar{Z}_S \end{bmatrix} \cdot \begin{bmatrix} \bar{I}_A \\ \bar{I}_B \\ \bar{I}_C \end{bmatrix} \quad (1)$$

where $\bar{V}_{\mathrm{RA}}$, $\bar{V}_{\mathrm{RB}}$, and $\bar{V}_{\mathrm{RC}}$ are the receiving-end phase voltages; $\bar{V}_{\mathrm{SA}}$, $\bar{V}_{\mathrm{SB}}$, and $\bar{V}_{\mathrm{SC}}$ are the sending end phase voltages; $\bar{I}_A$, $\bar{I}_B$, and $\bar{I}_C$ are the branch currents; and $\bar{Z}_S$ and $\bar{Z}_M$ are the self and mutual impedances, respectively.

When an SLG occurs, this equation can be rewritten in per unit as

$$\begin{bmatrix} \bar{V}_{\mathrm{RA}} \\ \bar{V}_{\mathrm{RB}} \\ \bar{V}_{\mathrm{RC}} \end{bmatrix} = \begin{bmatrix} 1\angle 0^\circ \\ 1\angle -120^\circ \\ 1\angle 120^\circ \end{bmatrix} - \begin{bmatrix} \bar{Z}_S & \bar{Z}_M & \bar{Z}_M \\ \bar{Z}_M & \bar{Z}_S & \bar{Z}_M \\ \bar{Z}_M & \bar{Z}_M & \bar{Z}_S \end{bmatrix} \cdot \begin{bmatrix} \bar{I}_A \\ 0 \\ 0 \end{bmatrix}. \quad (2)$$

Then, the short-circuit current in phase A is

$$\bar{I}_A = \frac{\bar{V}_{\mathrm{SA}} - \bar{V}_{\mathrm{RA}}}{\bar{Z}_S} = \frac{1\angle 0^\circ - 0}{\bar{Z}_S} = \frac{1}{\bar{Z}_S} \quad (3)$$

and the receiving end voltages are

$$\bar{V}_{\mathrm{RB}} = \bar{V}_{\mathrm{SB}} - \bar{I}_A \cdot \bar{Z}_M = 1\angle 120^\circ - \frac{1}{\bar{Z}_S} \cdot \bar{Z}_M \quad (4)$$

$$\bar{V}_{\mathrm{RC}} = \bar{V}_{\mathrm{SC}} - \bar{I}_A \cdot \bar{Z}_M = 1\angle -120^\circ - \frac{1}{\bar{Z}_S} \cdot \bar{Z}_M. \quad (5)$$

The last two expressions show that the voltages in the unfaulted phases depend on the complex ratio of mutual to self impedances.

When the resistive component is neglected, the ratio becomes a real number given by

$$\frac{\bar{Z}_M}{\bar{Z}_S} = \frac{jX_M}{jX_S} = \frac{X_M}{X_S}. \quad (6)$$

As a result, the phasors of the receiving end voltages V_{RB} and V_{RC} in (4) and (5) are equally displaced along the real axis in the complex plane as shown in Fig. 6(a). These voltage phasors are complex conjugate and their magnitudes are equal.

In the general case, when resistance is accounted for in the calculation, the impedance ratio is a complex number

$$\frac{\bar{Z}_M}{\bar{Z}_S} = \frac{R_M + jX_M}{R_S + jX_S} = \frac{\sqrt{R_M^2 + X_M^2}}{\sqrt{R_S^2 + X_S^2}} \angle \left[\tan^{-1}\left(\frac{X_M}{R_M}\right) - \tan^{-1}\left(\frac{X_S}{R_S}\right) \right]. \quad (7)$$

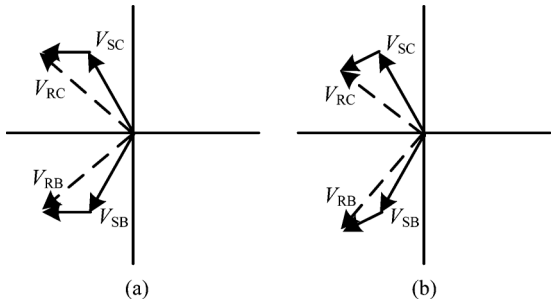

Fig. 6. Phasor diagram of overvoltages. (a) Considering reactance only. (b) Including resistance and reactance.

Thus, the receiving end voltages V_{RB} and V_{RC} will be equally displaced by $\sqrt{R_M^2 + X_M^2}/\sqrt{R_S^2 + X_S^2}$ in the direction defined by the angle difference in (7). This will cause voltages at the receiving end to be of different magnitudes as shown in Fig. 6(b).

The simplified analysis presented before explains why in further simulation results (just like in real-life measurements), the overvoltages in different phases of the distribution network are different during the SLG faults.

III. System Under Study

The network under investigation is supplied from an area substation that has seven transformers 132/25 kV, two capacitor banks, 15 bus breakers, and 12 feeder breakers (as shown in Fig. 1). The feeder breakers trip on instantaneous overcurrent of 4000 A peak, which added to the mechanical time delay, results in about 5 cycles of fundamental frequency in agreement with [25]. There are thousands of primary sections interconnected. These sections energize hundreds of network transformers of voltage 25/0.460 kV or 25/0.208 kV. Nearly 18 000 secondary mains sections are used to feed several thousands of nonuniformly distributed loads. We note, however, that the duration and magnitude of the overvoltages do not depend very much on the size of the network or number of nodes. Overvoltages exist for as long as there is a meshed secondary network where backfeeding can occur during a fault.

IV. Simulation Results

Simulations have been performed to illustrate severe long duration overvoltages occurring in a typical underground distribution network during SLG faults. These simulations consider in three cases of network loading: 1) peak load; 2) minimum load; and 3) no load. In every case, a short circuit has been applied in phase A on the primary side of a 1000-kVA 25/0.208-kV network transformer which is located at the end of one of the feeders as shown in Fig. 1.

It is assumed that the network operates initially in steady-state conditions and the fault occurs after approximately 3 cycles of the fundamental frequency (60 Hz) from the beginning of every simulation. The total length of all branches of the selected feeder is slightly larger than 7.6 km. These branches deliver a total charging power of 1624 kvar. The faulted area has 10 nearby network transformers connected to the grid.

To guard against operational failure of network protectors and to protect the interconnection of secondary mains, fuses and cable limiters are commonly used. These components are designed to blow or burn only on large current magnitudes lasting several seconds. Fuses and limiters are not modeled because they do not operate within the study time.

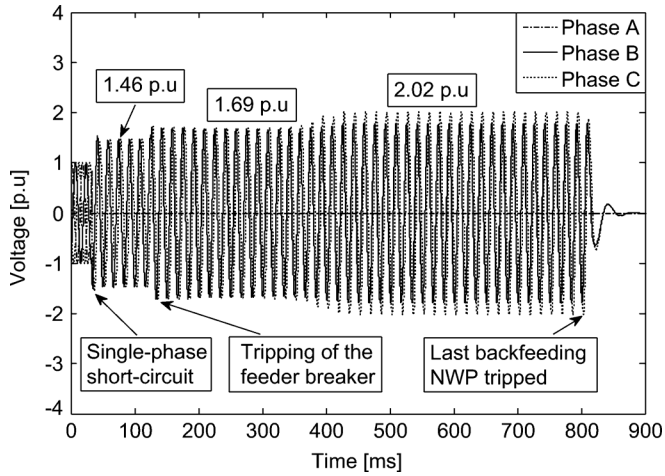

Fig. 7. Instantaneous voltage at the faulted transformer for the peak load case.

This study focuses on overvoltages. Therefore, a description of current behavior for each simulated case is omitted for the sake of brevity. However, it is important to indicate operational times of the feeder breaker in order to better understand the simulation results. For the presented cases, the smallest instantaneous fault current in the breaker is 4.8 kA. It exceeds the instantaneous overcurrent (IOC) settings (4 kA) of the device. As a result, the breaker opens in nearly six cycles after the fault and isolates the fault from the substation. Then, the network protectors along the feeder begin to trip, eventually achieving the complete isolation of the faulted feeder.

A. Network at Peak Load

The voltage waveform computed at the fault location for the peak load conditions is presented in Fig. 7. When the fault occurs (at 50 ms), the reference to ground is still present in the primary network, and the voltages of the unfaulted phases do not exceed 1.46 p.u. After the breaker trips at 136 ms, the feeder remains energized only by reverse power flow and the voltages rise to 1.69 p.u. At this point, the overvoltages do not reach a theoretical value of $\sqrt{3}$ p.u. because of the large loading of the secondary grid which still remains electrically connected to the faulted feeder. As a consequence of the gradual operation of the network protectors, the overvoltage increases. Indeed, the voltages in phases B and phase C reach 1.78 and 2.02 p.u., respectively. The significant difference in the values of these voltages is due to the high R/X ratio of the distribution network as explained in Section II. The total time of the overvoltage extends to approximately 42 cycles. It should be noted that when a large portion of the network protectors disconnects, the feeder loading decreases enough for the Ferranti effect to occur and raise the voltages above the line-to-line level.

B. Network at Minimum Load

The instantaneous voltage waveforms at the fault location for the lightly loaded network are given in Fig. 8. Analyzing these

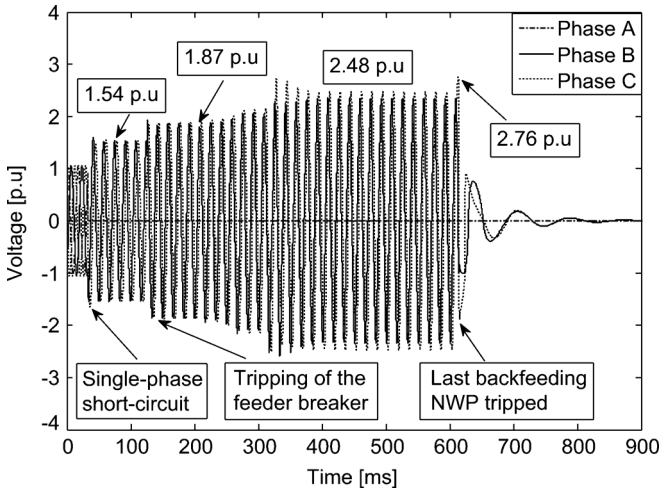

Fig. 8. Instantaneous voltage at the faulted transformer for the light load case.

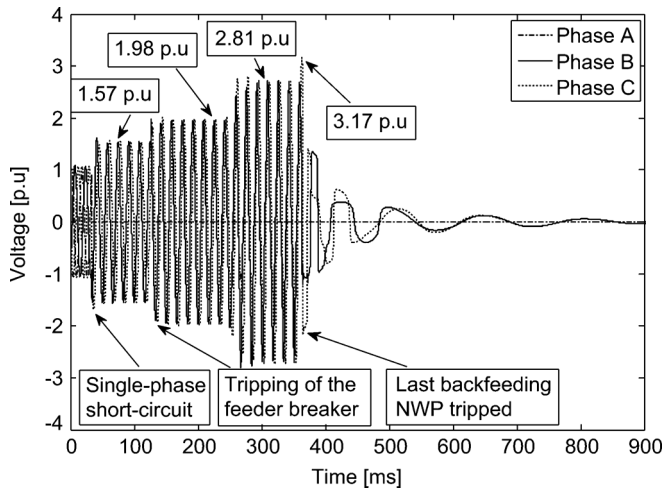

Fig. 9. Instantaneous voltage at the faulted transformer for the no-load case.

waveforms, one may notice that for the light network loading, the overvoltages are of larger magnitude than those reported for the peak loading. The obtained results illustrate that the voltages of the unfaulted phases at the fault location reach 1.54 p.u. and remain at this value for 5 cycles until right before the short circuit is disconnected from the substation at 136 ms. After the breaker and several network protectors open, the voltage magnitudes rise to 2.48 p.u. due to the Ferranti effect. The Ferranti effect persists for approximately 30 cycles until the last network protector trips and isolates the feeder at approximately 615 ms. It should be noted that the Ferranti effect is noticeable in this case, right from the tripping of the breaker, because the network loading is relatively small. Furthermore, when the last LV protective device opens, chopping the backfeeding current, the transient voltage rises to 2.76 p.u. as a result of the underdamped network behavior which may be potentially harmful to electrical equipment.

C. Network at No Load

Simulation results of the network having no load provide an insight of what would be the worst case scenario regarding magnitudes of transient overvoltages caused by an SLG fault. In the absence of loads in the LV grid, all current in the nearby secondary area will backfeed to the fault through the network transformers causing their network protectors to trip at a faster rate than in the cases where there is load connected to the network. In the no-load case, the feeder breaker trips at approximately 5 cycles after the fault occurrence. Fig. 9 shows voltage waveforms at the fault location. In this figure, voltages of the unfaulted phases are equal to 1.57 p.u. during the initial phase of the fault. After the breaker opening at 136 ms, there is a voltage rise to 1.98 p.u. The voltages in the unfaulted phases continue to increase further up to 2.81 p.u. as several network protectors open.

Here, voltage rises resulting from the Ferranti effect last for approximately 15 cycles after the breaker opens. After the disconnection of the last network protector, the chopping of the backfeeding current causes a significant transient overvoltage of 3.17 p.u., which appears at the fault location as shown in Fig. 9.

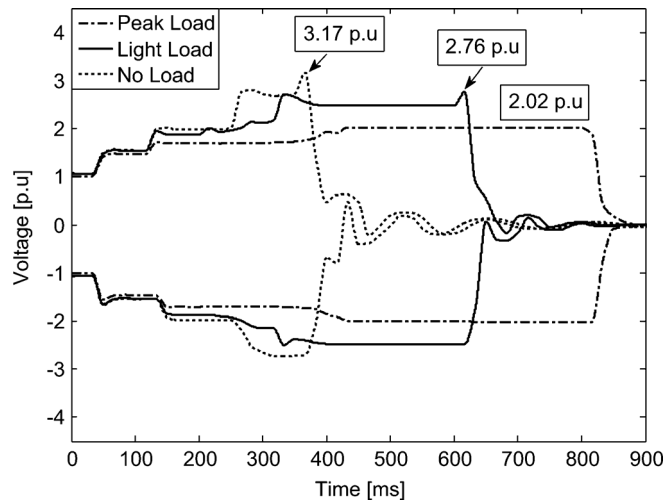

Fig. 10. Comparison of envelopes for each resulting voltage waveform measured at the fault location.

The magnitude of this voltage spike is the largest among the presented simulation cases.

D. Comparison of Simulation Results

To facilitate the comparison between simulated cases, the envelopes for the resulting voltage waveforms at the fault location are provided in Fig. 10. The outcomes of the simulations reveal that the worst case scenario occurs during no-load conditions with 3.17 p.u. of transient overvoltage at the instant of disconnection of the last network protector. Furthermore, it was observed that for all cases, after the breaker of the faulted feeder opens, overvoltages exceed the theoretical neutral displacement value of $\sqrt{3}$ p.u. due to the Ferranti effect.

The duration of the overvoltages depends on the system load. There is a direct impact of the network loading on the overvoltage severity. For the unloaded case, network protectors trip relatively fast as the backfeeding conditions are immediately satisfied. As a result, the time interval required for the network to withstand the overvoltages is reduced. However, for loaded cases, the network consumption must be supplied even if there

TABLE I
COMPARISON OF OVERVOLTAGES DUE TO SINGLE-LINE-TO-GROUND FAULTS

Case/Period	Fault [p.u.]	Breaker Open [p.u.]	Spike [p.u.]
Peak Load	1.46	2.02	--
Light Load	1.54	2.48	2.76
No Load	1.57	2.81	3.17

is a fault present on a feeder. This fact results in smaller backfeeding currents leading to extended overvoltages. Table I summarizes the network voltages for each simulated case during different transient periods. Even though the unloaded case manifests the worst case scenario, it is unlikely for networks to be unloaded in urban areas (probably during restoration only). Therefore, the more realistic minimum load conditions are selected to demonstrate two techniques of overvoltage mitigation.

V. MITIGATION OF OVERVOLTAGES

In this section, two methods of overvoltage mitigation are studied. The first method is based on reactive power compensation by means of shunt reactors. The second one exploits grounding transformers to provide a ground reference to the system after CB tripping in the substation. These solutions are aimed to mitigate the Ferranti effect and to limit or eliminate completely the spike produced by the underdamped behavior of the remaining circuit after disconnection of the last network protector. The simulation results demonstrate the effects of the following: 1) full compensation of the faulted feeder charging power by means of a shunt reactor rated 1624 kvar connected at the end of the line, near the fault location and 2) insertion of a grounding transformer (connected in zigzag) with equivalent zero-sequence impedance of 15 Ω selected in accordance with [26].

A. Single-Phase Fault Mitigated With a Shunt Reactor

One of the most common devices for reducing overvoltages is a shunt reactor. In urban areas where underground cables are installed, it is used to compensate the charging power of long distribution feeders, especially during backfeeding conditions. In underground cable systems, there is substantial capacitance to ground similar to that of a long overhead line. The cables operate below their surge impedance loading and, therefore, shunt reactors help maintain a desirable voltage profile. As previously discussed, during a single-phase fault, the network phase voltage might reach or even exceed the line-to-line value due to displacement of the neutral reference and the Ferranti effect. For the cases presented in this paper, the aim of the shunt reactor is to reduce overvoltages after the substation grounding point is disconnected from the faulted feeder.

To determine the size of the reactor, theoretical analysis is performed considering the equivalent state of the faulted feeder before the tripping of the last network protector (see Fig. 11). The series impedance of the feeder is significantly smaller than the leakage impedances of the backfeeding network transformers. Therefore, the line impedance can be neglected for this analysis (however, it is included in the simulations). At this stage, it can be seen that the location of the shunt reactor along the faulted feeder is irrelevant provided that a ground reference

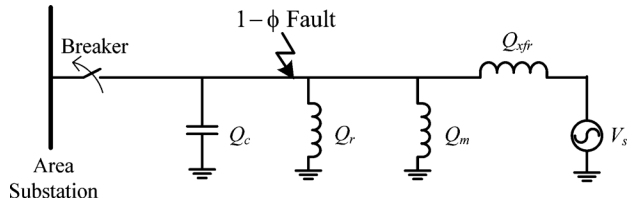

Fig. 11. Simplification of the network to illustrate overvoltage mitigation using a shunt reactor.

is provided. This is so because there is no significant change in voltage between the branches of the MV line. Q_c represents the total charging vars of the feeder, Q_m corresponds to the excitation vars of the disconnected transformers, and Q_r is the shunt reactor. Q_m obtained using individual nonlinear magnetizing curves of the network transformers for 10% voltage rise on the grid side, which is the emergency operating condition per standards [27], [28]. The value of Q_r has been selected in such a way that, together with Q_m, it compensates for 100% of Q_c in all sequences (positive, negative, and zero) during an SLG fault.

This simulation case shows that the overvoltages are mitigated during an SLG fault using a shunt reactor that fully compensates capacitive charging power. The instantaneous voltage waveforms at the fault location are given in Fig. 12. The voltages before isolation of the substation at 136 ms are 1.54 p.u. After the breaker trips, the voltages rise to 1.77 p.u. due to the Ferranti effect produced by the current backfeeding. This indicates a significant improvement (28.6% of reduction) compared to the case without shunt reactors where the voltages reached 2.48 p.u. It should be noted that the transient overvoltage spike after the disconnection of the last network protector is not observed when the shunt reactors are connected.

B. Single-Phase Fault Mitigated With a Grounding Zigzag Transformer

Another commonly used option for reducing overvoltages is providing a neutral reference after the substation grounding point is disconnected from the faulted feeder. For this purpose, a grounding transformer connected in zigzag is utilized. As opposed to the shunt reactor, the grounding transformer does not affect normal system operation since it has very high positive- and negative-sequence impedances. At the same time, its zero-sequence impedance is low. Thus, the grounding transformer provides a low-impedance path to ground only during unbalanced conditions of the network.

The behavior of voltage at the fault location when a grounding transformer installed in the network is shown in Fig. 13. As can be seen in this figure, the voltages before disconnection of the substation at 136 ms are 1.48 p.u. After the feeder breaker trips and several energized transformers are gradually disconnected by their network protectors, voltages in phases B and C reduce to 1.09 p.u. and 0.91 p.u., respectively. It should be noted that without the grounding transformer, installed, these voltages were significantly higher (1.54 p.u. before the feeder breaker tripping and 2.48 p.u., after). By using the grounding transformer, a path to ground has been provided in the distribution network. This greatly reduces the

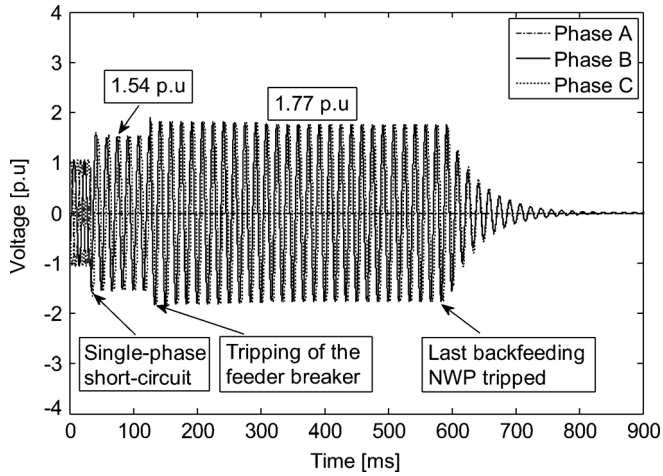

Fig. 12. Instantaneous voltage at the fault location mitigated using a shunt reactor.

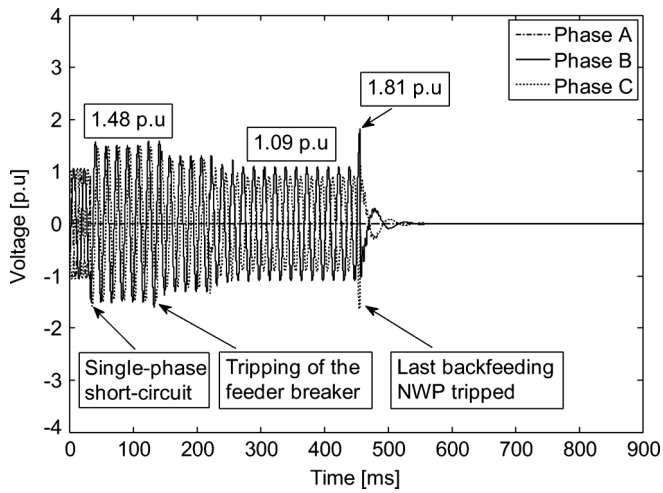

Fig. 13. Instantaneous voltage at the fault location mitigated using a grounding transformer with zigzag connection.

displacement of the neutral and limits the overvoltage to only about 10% of nominal voltage. In addition, the simulation results show that the grounding transformer significantly reduces the transient overvoltage after the opening of the last network protector. Indeed, the magnitude of the voltage spike was 2.76 p.u. without the grounding transformer. However, when such a transformer has been connected, the voltage spike reaches only 1.81 p.u. (i.e., a reduction of 34.4% has been achieved).

According to the findings presented before, it is concluded that grounding transformers provide an effective method for overvoltage reduction during SLG faults. Indeed, in comparison with the case without the grounding transformer, its installation has reduced steady-state overvoltages during the fault by 56.1% and transient overvoltages by 34.4%.

C. Comparison of Results For Mitigation Schemes

In this paper, it has been determined that grounding transformers have advantages over shunt reactors in mitigation of the overvoltages caused by SLG faults. These transformers successfully eliminate voltage rise due to neutral displacement, Ferranti effect, as well as shortening the duration of overvoltages after isolation of the substation grounding. Furthermore, it greatly

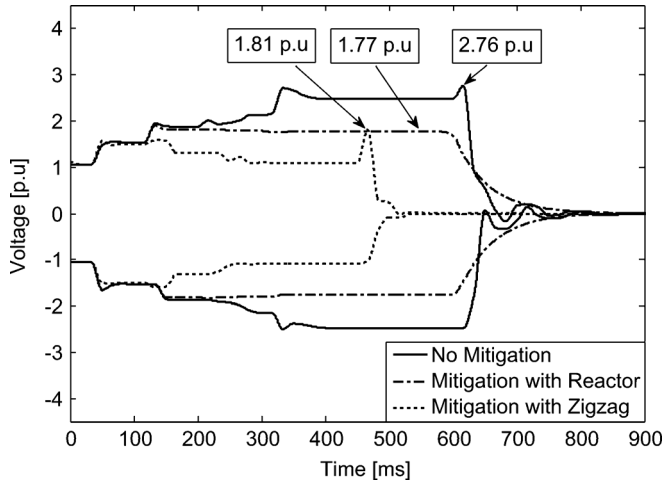

Fig. 14. Comparison of envelopes for each of resulting voltages under different mitigation schemes.

TABLE II
COMPARISON OF THE OVERVOLTAGES DUE TO SINGLE-LINE-TO-GROUND FAULTS UNDER DIFFERENT MITIGATION SCHEMES

Case/Period	Fault [p.u.]	Breaker Open [p.u.]	Spike [p.u.]	Total Time [ms]
Base Case	1.54	2.48	2.76	615
Shunt Reactor	1.54	1.77	1.77	600
Grounding Transformer	1.48	1.09	1.81	475

reduces the voltage spikes after disconnection of the last network protector on the faulted feeder. Table II provides a summary of the calculated voltages at different stages of the SLG fault isolation for the light load cases with and without overvoltage-mitigating devices. A graphical comparison of the instantaneous voltage envelopes obtained at the fault location is given in Fig. 14.

In the case of the shunt reactor installation, the Ferranti effect is significantly reduced. The voltages do not rise above 2.0 p.u. However, they still exceed 1.73 p.u. This mitigation technique also eliminates the transient overvoltages.

When the grounding transformer is used, the possibility of overvoltages exceeding 1.73 p.u. is greatly reduced since an alternative grounding reference to the system is provided. It was shown by means of the time-domain simulations that grounding transformers can reduce the possible transient overvoltages that occurred after disconnection of the last network protector on the faulted feeder.

Similar studies were performed on a 34.5-kV feeder of another real-size network. The simulation results and conclusions are in agreement with those reported for the 25-kV systems in this paper.

VI. CONCLUDING REMARKS

This paper has presented for the first time a study on long duration overvoltages in heavily meshed underground distribution networks. The duration of these overvoltages was found to be longer for peak loading conditions. By means of time-domain simulations in the EMTP, it was proven that backfeeding from the secondary grid to the primary network raises voltages above

the theoretical neutral displacement value of $\sqrt{3}$ p.u. due to the Ferranti effect. Also, it was discovered that during disconnection of the last network protector, a very large voltage spike is produced due to current chopping. The magnitude of this spike exceeds 3 p.u. when the network is lightly loaded.

The observed voltage magnitudes may cause damage to insulation of the distribution network equipment. To prevent their occurrence, a thorough analysis of overvoltages during unbalanced faults is necessary and the application of grounding transformers or shunt reactors is highly recommended. The comparison of these two overvoltage mitigation methods has shown the grounding transformer to be more effective for mitigating overvoltages during single-line-to-ground faults.

REFERENCES

[1] *Electrical Transmission and Distribution Reference Book*. East Pittsburgh, PA: Westinghouse Electric Corp, 1964.

[2] *IEEE Standard Requirements for Secondary Network Protectors*, IEEE Standard C57.12.44, 2005.

[3] W. J. Lee, J. Cultrera, and T. Maffetone, "Application and testing of a microcomputer based network protector," *IEEE Trans. Ind. Appl.*, vol. 36, no. 2, pp. 691–696, Mar./Apr. 2000.

[4] V. Spitsa, R. Salcedo, X. Ran, J. Martinez, R. Uosef, F. d. León, D. Czarkowski, and Z. Zabar, "Three-phase time-domain simulation of very large distribution networks," *IEEE Trans. Power Del.*, vol. 27, no. 2, pp. 677–687, Apr. 2012.

[5] V. Spitsa, X. Ran, R. Salcedo, J. Martinez, R. Uosef, F. d. León, D. Czarkowski, and Z. Zabar, "On the transient behavior of large-scale distribution networks during automatic feeder reconfiguration," *IEEE Trans. Smart Grid*, vol. 3, no. 2, pp. 887–896, Jun. 2012.

[6] P. Chen, R. Salcedo, Q. Zhu, F. d. León, D. Czarkowski, Z. P. Jiang, V. Spitsa, Z. Zabar, and R. Uosef, "Analysis of voltage profile problems due to the penetration of distributed generation in low-voltage secondary distribution networks," *IEEE Trans. Power Del.*, vol. 27, no. 4, pp. 2020–2028, Oct. 2012.

[7] M. Diaz-Aguiló, J. Huang, F. d. León, D. Czarkowski, and J. Mahseredjian, "Probabilistic analysis of fault induced delayed recovery voltage," *IEEE Trans. Power Del.*, submitted for publication.

[8] W. E. Feero and W. B. Gish, "Overvoltages caused by dsg operation: synchronous and induction generators power delivery," *IEEE Trans. Power Del.*, vol. PWRD-1, no. 1, pp. 258–264, Jan. 1986.

[9] Q. Sun, Z. Li, and H. Zhang, "Impact of distributed generation on voltage profile in distribution system," in *Proc. Int. Joint Conf. Comput. Sci. Optimiz.*, 2009, pp. 249–252.

[10] P. Barker, "Overvoltage considerations in applying distributed resources on power systems," in *Proc. IEEE Power Eng. Soc. Summer Meeting*, 2002, vol. 1, pp. 109–114.

[11] S. A. Ali, "Capacitor banks switching transients in power systems," *Energy Sci. Technol.*, vol. 2, no. 2, pp. 62–73, Nov. 2011.

[12] S. Silfverskiold, R. Thottappillil, M. Ye, V. Cooray, and V. Scuka, "Induced voltages in a low-voltage power installation network due to lightning electromagnetic fields: an experimental study," *IEEE Trans. Electromagn. Compat.*, vol. 41, no. 3, pp. 265–271, Aug. 1999.

[13] A. Galvan, V. Cooray, and R. Thottappillil, "A technique for the evaluation of lightning-induced voltages in complex low-voltage power-installation networks," *IEEE Trans. Electromagn. Compat.*, vol. 43, no. 3, pp. 402–409, Aug. 2001.

[14] A. Borghetti, A. Morched, F. Napolitano, C. A. Nucci, and M. Paolone, "Lightning-induced overvoltages transferred through distribution power transformers," *IEEE Trans. Power Del.*, vol. 24, no. 1, pp. 360–372, Jan. 2009.

[15] H. Shareef, S. N. Khalid, M. W. Mustafa, and A. Mohamed, "Modeling and simulation of overvoltage surges in low voltage systems," in *Proc. 2nd IEE Int. Power and Energy Conf.*, 2008, pp. 357–361.

[16] J. Orsagova and P. Toman, "Transient overvoltages on distribution underground cable inserted in overhead line," presented at the 20th Int. Conf. Exhibit. Elect. Distrib., Prague, Czech Republic, Jun. 8–11, 2009.

[17] M. M. Adibi, R. W. Alexander, and B. Avramovici, "Overvoltage control during restoration," *IEEE Trans. Power Syst.*, vol. 7, no. 4, pp. 1464–1470, Nov. 1992.

[18] S. Chen and H. Yu, "A review on overvoltages in microgrid," in *Proc. Power Energy Eng. Conf. Asia-Pacific*, Mar. 2010, pp. 28–31.

[19] J. P. Bickford and A. G. Heaton, "Transient overvoltages on power systems," *Proc. Inst. Elect. Eng.*, vol. 133, no. 4, pp. 201–225, May 1986.

[20] A. Cerretti, F. M. Gatta, A. Geri, S. Lauria, M. Maccioni, and G. Valtorta, "Ground fault temporary overvoltages in MV networks: Evaluation and experimental tests," *IEEE Trans. Power Del.*, vol. 27, no. 3, pp. 1592–1600, Jul. 2012.

[21] R. A. Walling and R. D. Melchior, "Measurement of cable switching transients in underground distribution systems," *IEEE Trans. Power Del.*, vol. 10, no. 1, pp. 534–539, Jan. 1995.

[22] DCG-EMTP (Development Coordination Group of EMTP) Version EMTP-RV, Electromagnetic Transients Program. [Online]. Available: http://www.emtp.com

[23] J. C. Das, *Power System Analysis-Short-Circuit, Load Flow and Harmonics*. New York: Marcel Dekker, 2002, p. 346.

[24] A. Greenwood, *Electrical Transients in Power Systems*, 2nd ed. New York: Wiley, 1991, pp. 92–100.

[25] *IEEE Standard for AC High-Voltage Circuit Breakers Rated on a Symmetrical Current Basis-Preferred Ratings and Related Required capabilities for Voltages Above 1000 V* , IEEE Standard C37.06, 2009.

[26] *IEEE Guide for the Application of Neutral Grounding in Electrical Utility Systems, Part IV—Distribution*, IEEE C62.92.4, 1991.

[27] *IEEE Standard for Interconnecting Distributed Resources With Electric Power Systems*, IEEE Standard 1547, 2003.

[28] *Voltage Ratings for Electric Power Systems and Equipment National Electrical Manufacturers Association (NEMA)*, American National Standards Institute (ANSI) C84.1-2006, 2006.

Reynaldo Salcedo (S'09) received the B.Sc. and M.Sc. degrees in electrical engineering from Polytechnic Institute of New York University, Brooklyn, NY, USA, in 2011 and 2012, respectively, where he is currently pursuing the Ph.D. degree in electrical engineering.

His research interests include electromagnetic transient analysis in power systems and power system modeling and analysis.

Xuanchang Ran received the B.Sc. degree in electrical engineering from Southwest Jiaotong University, Chengdu, China, in 2008, and the M.Sc. degree in electrical engineering from Polytechnic Institute of New York University, Brooklyn, NY, USA, in 2010, where he is currently pursuing the Ph.D. degree.

His research interest is power system analysis and power theory research.

Francisco de León (S'86–M'92–SM'02) received the B.Sc. and the M.Sc. (Hons.) degrees in electrical engineering from the National Polytechnic Institute, Mexico City, Mexico, in 1983 and 1986, respectively, and the Ph.D. degree in electrical engineering from the University of Toronto, Toronto, ON, Canada, in 1992.

He has held several academic positions in Mexico and has worked for the Canadian electric industry. Currently, he is an Associate Professor at the Polytechnic Institute of New York University, Brooklyn, NY, USA. His research interests include the analysis of power definitions under nonsinusoidal conditions, the transient and steady-state analyses of power systems, the thermal rating of cables and transformers, and the calculation of electromagnetic fields applied to machine design and modeling.

Dariusz Czarkowski (M'97) received the M.Sc. degree in electronics from the University of Mining and Metallurgy, Krakow, Poland, in 1989, the M.Sc. degree in electrical engineering from Wright State University, Dayton, OH, USA, in 1993, and the Ph.D. degree in electrical engineering from the University of Florida, Gainesville, FL, USA, in 1996.

In 1996, he joined the Polytechnic Institute of New York University, Brooklyn, NY, where he is currently an Associate Professor of Electrical and Computer Engineering. He is a coauthor of *Resonant Power Converters* (Wiley Interscience, 2011). His research interests are in the areas of power electronics, electric drives, and power quality.

Dr. Czarkowski has served as Associate Editor for the IEEE TRANSACTIONS ON CIRCUIT AND SYSTEMS.

Vitaly Spitsa (M'10) received the M.Sc. and Ph.D. degrees in electrical engineering from Technion—Israel Institute of Technology, Haifa, Israel, in 2002 and 2009, respectively.

He has been a Control and Algorithm Engineer with a motion control company in Israel. Currently, he is a Research Assistant Professor at Polytechnic Institute of New York University, Brooklyn, NY, USA. His research interests are in the areas of power system analysis, electrical machines, drives, and robust control.